

## Supporting Information

Sarmimala Hore,<sup>\*a</sup> Gerhard Kaiser,<sup>b</sup> Yong-Sheng Hu,<sup>a</sup>  
Armin Schulz,<sup>a</sup> Mitsuharu Konuma,<sup>a</sup> Gabriele Götz,<sup>a</sup>  
Wilfried Sigle,<sup>b</sup> Aswin Verhoeven,<sup>a</sup> and Joachim  
Maier<sup>a</sup>

### Materials and Methods

Typically the  $\text{Au}_2\text{O}_3$ /polymer blends were made by adding  $\text{Au}_2\text{O}_3 \cdot x\text{H}_2\text{O}$  (Aldrich) and polyethylene(PE) (Aldrich, 81219) or poly-vinylidene fluoride(PVDF) 90:10 by weight. PE was added to toluene and heated to  $80^\circ\text{C}$ , and once the polymer is dissolved and dispersed in toluene, it is added to the  $\text{Au}_2\text{O}_3$  using a mortar and pestle. PVDF is usually added to N-methyl pyrrolidone at a temperature of  $60^\circ\text{C}$  and stirred for up to 8 h to make a homogeneous solution and is then added to the  $\text{Au}_2\text{O}_3$ . Once the blends with  $\text{Au}_2\text{O}_3$ /polymer are made, they were pasted on Ti or Cu foils and dried under IR lamp and then heated using a vacuum oven at  $80^\circ\text{C}$  for 8 h.

Micro Raman Spectra were recorded on a Jobin Yvon Lab Ram micro-Raman spectrometer with an excitation wavelength of 632.8 nm, and the laser power ranging from 0.04 – 2 mW, the spotsize being 20  $\mu\text{m}$  at the sample. HRTEM images were collected by using a JEOL 2000EX (operating at 200 kV) and a JEOL 4000EX (operating at 400 kV) transmission electron microscope, respectively. XRD measurements were carried out in Bragg-Brentano-geometry with a PHILIPS PW3710 using filtered  $\text{Cu K}\alpha$  radiation. NETZSCH STA 449C was used to perform thermogravimetry and differential calorimetry measurements at a heating rate of  $3^\circ/\text{min}$  in Ar flow, and mass spectrometry (MS) was carried out using quadrupole spectrometer (IPI GAM 200). The DSC/MS was carried out using solid state samples i.e. polymers and powdered  $\text{Au}_2\text{O}_3$  mixed without any solvent. The thermogravimetry shows weight loss for all the systems whenever there was an evolution of reaction gases (reaction of  $\text{Au}_2\text{O}_3$  and polymers). However, the weight loss was not quantified with respect to the production of the gaseous species.

The NMR data were acquired on a 9.4 T Bruker DSX spectrometer employing a 4 mm TR probe (operating in DR mode). The chemical shift axis was calibrated with an adamantane sample ( $\delta\text{CH}_2 = 37.9$  ppm). The spectra were acquired using a rotor-synchronous Hahn-echo pulse sequence to suppress background signal and deadtime effects. This was combined with continuous-wave proton decoupling. The RF field amplitude was 25 kHz for  $^{13}\text{C}$  and 56 kHz for  $^1\text{H}$ . The magic-angle spinning (MAS) frequency was 14 kHz. 2160 scans were accumulated with a relaxation delay of 30 s. X-ray photoelectron spectroscopy was performed on an electron spectrometer (AXIS ULTRA, Kratos) by use of monochromatized  $\text{Al K}\alpha$  radiation (1486.58 eV). The vacuum during the measurements was kept below  $3 \times 10^{-9}$  Torr. The sample surfaces were sputtered with high purity argon for 5 min. To account for charging, the spectra were calibrated with respect to an internal  $\text{C}(1s)$  line (binding energy of 285.0 eV). The peak profiles were fitted with a Voigt function.

As an internal standard, spectrum was taken first from gold foil.

### Figures

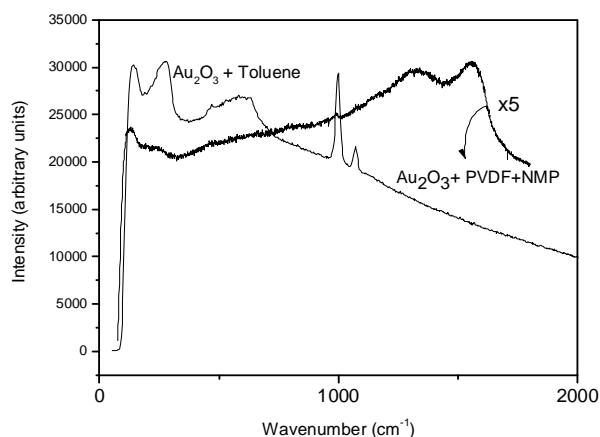


**Figure S1.** Raman spectra of ( $\text{Au}_2\text{O}_3 + \text{Toluene}$ ) and ( $\text{Au}_2\text{O}_3 + \text{PVDF} + \text{NMP}$ ) and the solvent was allowed to slowly evaporate at  $80^\circ\text{C}$  and at room temperature respectively. Formation of carbon was not observed in case of toluene and is most likely due to the evaporation of toluene prior to the evolution of nascent oxygen from  $\text{Au}_2\text{O}_3$ . The role of nascent oxygen will be discussed later on the in the text. The Raman spectrum of pure  $\text{Au}_2\text{O}_3$  has identical modes as that of the spectra labelled ( $\text{Au}_2\text{O}_3 + \text{Toluene}$ ). The Raman modes are 143.6, 273.1, broad feature around 580, 999.1 and  $1071.5 \text{ cm}^{-1}$ . The D and the G bands are respectively at 1320 and  $1555 \text{ cm}^{-1}$ . The laser intensity at the excitation wavelength of 632 nm was  $0.13 \text{ kW}/\text{cm}^2$ .

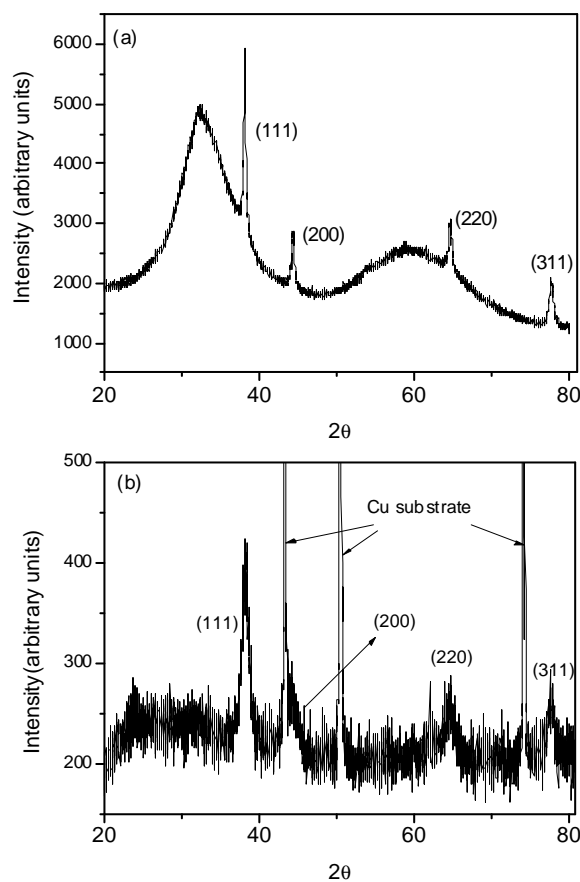


**Figure S2.**  $\text{Cu K}\alpha$  - Powder diffraction of  $\text{Au}_2\text{O}_3$ . (a)  $\text{Au}_2\text{O}_3 \cdot x\text{H}_2\text{O}$  (as received from Aldrich). (b)  $\text{Au}_2\text{O}_3$  blended with PVDF and NMP on a

copper support. The (111), (200), (220) and (311) reflections of metallic gold are indicated in the figure.

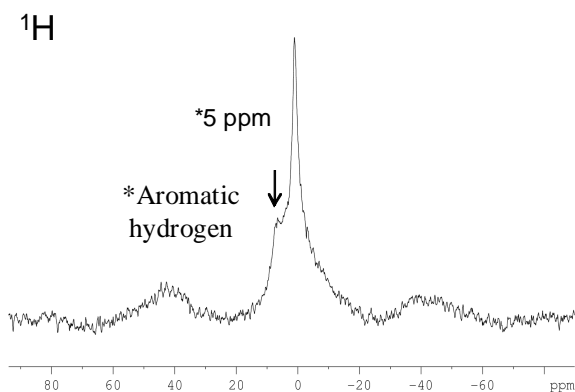


Figure S3. Solid state  $^1\text{H}$  NMR of  $\text{Au}_2\text{O}_3/\text{PE}$

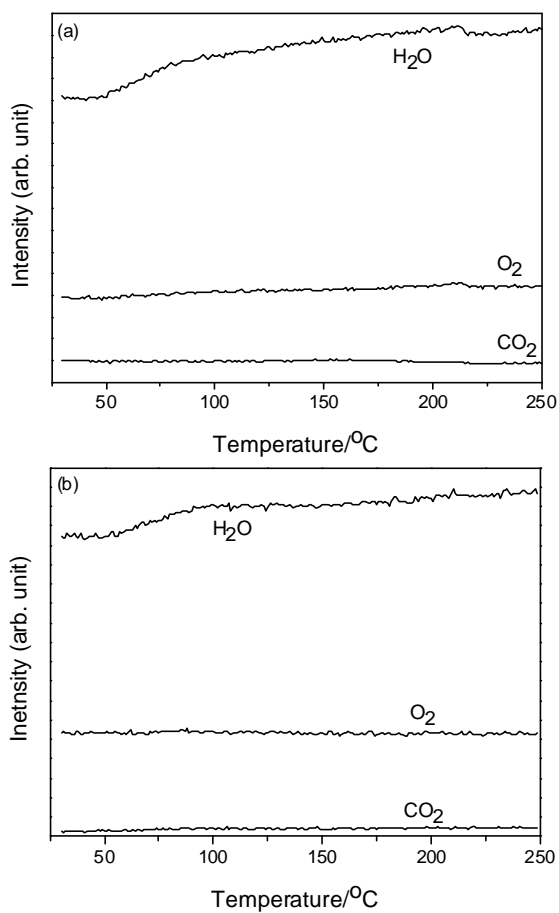


Figure S4. MS ion current of  $\text{CO}_2$ ,  $\text{H}_2\text{O}$  and  $\text{O}_2$  while heating (a)  $\text{Au}_2\text{O}_3$  and (b) PE.

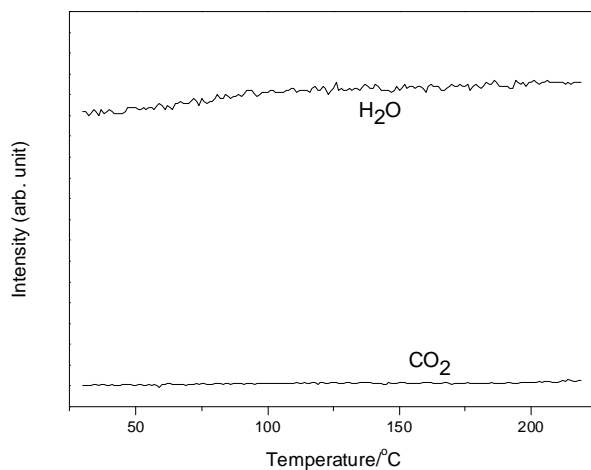


Figure S5. MS ion current of  $\text{H}_2\text{O}$  and  $\text{CO}_2$  when PE was heated in 500 ppm of  $\text{O}_2$  (in Ar). Only the melting of PE was observed in the DSC.

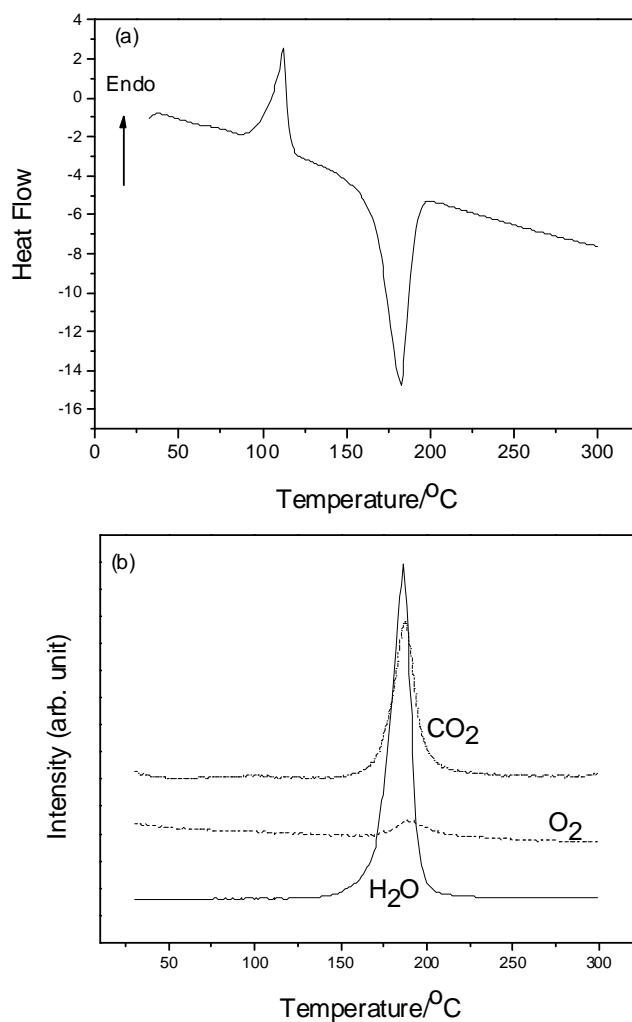
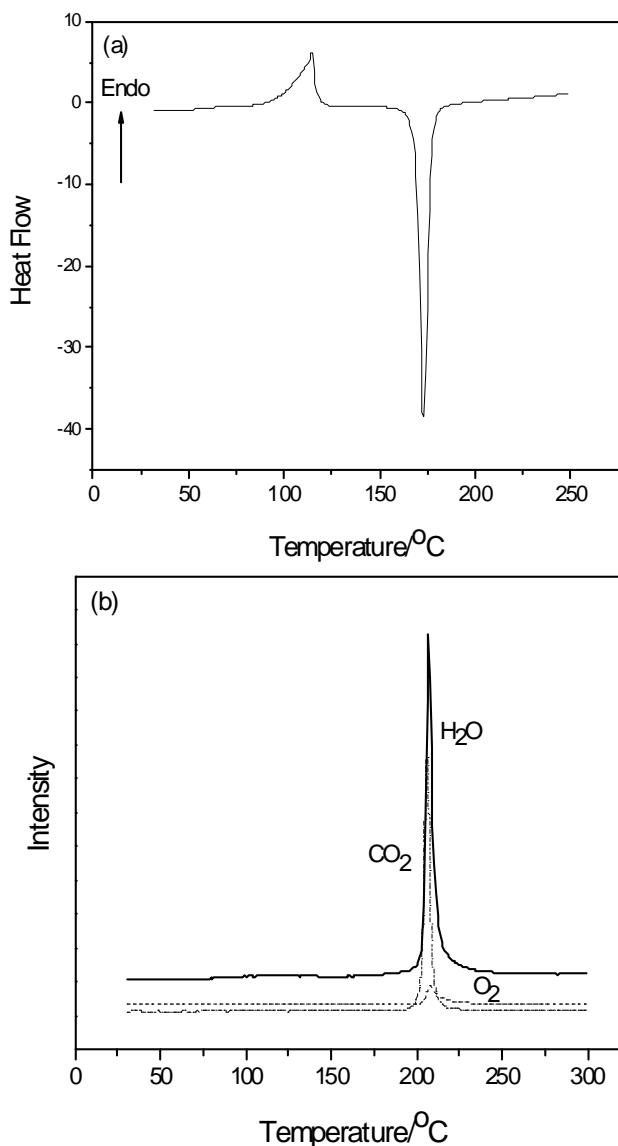


Figure S6. (a) DSC (in Ar) indicating melting of PE and the solid state exothermic reaction of  $\text{Ag}_2\text{O}$  and PE (b) MS ion current of  $\text{CO}_2$ ,  $\text{H}_2\text{O}$  and  $\text{O}_2$  during this process.



**Figure S7.** (a) DSC (in Ar) indicating melting of PE and the solid state exothermic reaction of  $\text{PtO}_2$  and PE (b) MS ion current of  $\text{CO}_2$ ,  $\text{H}_2\text{O}$  and  $\text{O}_2$  during this process.

5

In all these cases, whether the reaction proceeds in presence of  $\text{Au}_2\text{O}_3$ ,  $\text{Ag}_2\text{O}$  or  $\text{PtO}_2$ , the formation of  $\text{CO}_2$  and  $\text{H}_2\text{O}$  occurs concurrently. The only difference in case of  $\text{Au}_2\text{O}_3$  is the occurrence of the exothermic reaction in several stages and the onset of the reaction is lower than that of the reactions with  $\text{Pt}_2\text{O}$  or  $\text{Ag}_2\text{O}$ .

10

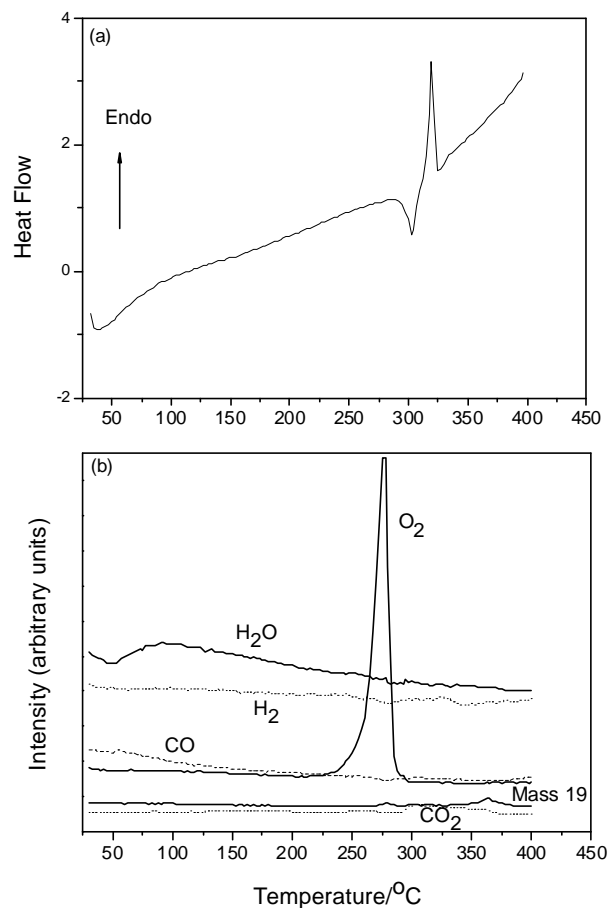


**Figure S8.** (a) DSC (in Ar) indicating melting of PTFE and the solid state exothermic reaction of  $\text{Au}_2\text{O}_3$  with PTFE (b) MS ion current of  $\text{CO}_2$ ,  $\text{H}_2\text{O}$ ,  $\text{O}_2$ ,  $\text{CO}$ , and mass 19.

PTFE melts between  $310 - 320^\circ\text{C}$  and since  $\text{Au}_2\text{O}_3$  decomposes earlier than the melting of the PTFE, we observe the beginning of the exothermic reaction as soon as the PTFE becomes soft and before the actual melting temperature for PTFE is reached. The mass spectrometer signal at atomic mass unit (amu) 19 is indicative of the presence of fluorine (18.998 amu). Due to the reaction of  $\text{Au}_2\text{O}_3$  on PTFE, we have observed the presence of fluorine occurring simultaneously with the formation of the oxygen peak at  $275^\circ\text{C}$  (Fig.S9 - S11). Often the signal at mass 19 is associated with the hydronium ion ( $\text{H}_3\text{O}^+$ ). Since there is no release of  $\text{H}_2\text{O}$  during the above reaction between PTFE and  $\text{Au}_2\text{O}_3$ , the mass 19 signal is not due to  $\text{H}_3\text{O}^+$ . Simultaneous release of oxygen and fluorine is indicative of the freshly formed oxygen species being responsible for the disintegration of the PTFE. Mass 19 and  $\text{CO}_2$  are shown in higher magnification in Fig. S9.

35

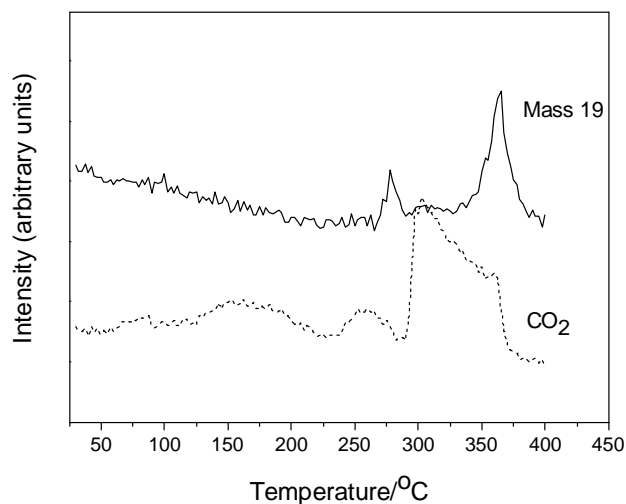


**Figure S9.** Release of CO<sub>2</sub> and mass 19 when Au<sub>2</sub>O<sub>3</sub> reacts with PTFE.

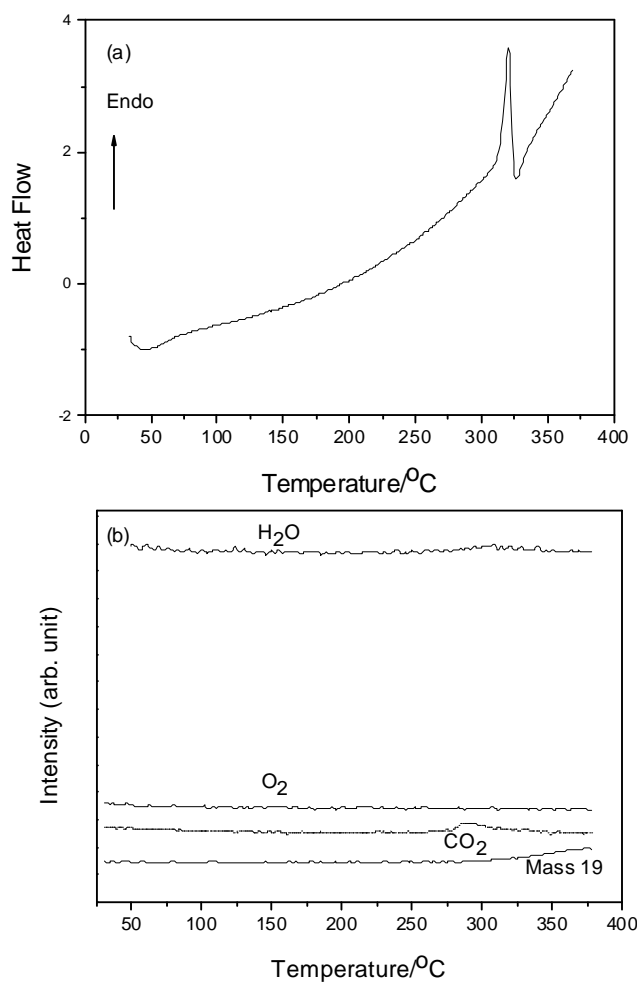


**Figure S10.** (a) DSC indicating melting of PTFE and the solid state exothermic reaction of PtO<sub>2</sub> with PTFE (b) MS ion current of CO<sub>2</sub>, H<sub>2</sub>O, O<sub>2</sub> and mass 19 during this process.

In case of the reaction of PtO<sub>2</sub> with PTFE, we observe that the exothermic reaction starts after the melting of PTFE. In this case the oxygen peak is not observed because either the formation of the CO<sub>2</sub> has consumed the evolved oxygen, or, the decomposition of PtO<sub>2</sub> is not complete. The amount of CO<sub>2</sub> release is much higher in case of the reaction with PtO<sub>2</sub>, compared to that of the reaction with Au<sub>2</sub>O<sub>3</sub> (Fig. S12). Here, however, no attempt has been made to quantify the amounts of the reaction products. For consistency, equal molar numbers of Au<sub>2</sub>O<sub>3</sub> and that of PtO<sub>2</sub> had been utilized.

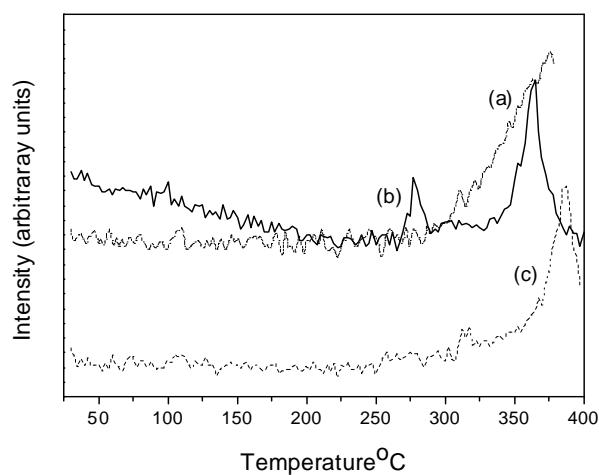


**Figure S11.** Mass spectrometer signal at atomic mass unit 19, indicating the presence of fluorine due to the reaction of PTFE with (a) PtO<sub>2</sub>, (b) Au<sub>2</sub>O<sub>3</sub> and (c) PTFE is heated without any oxide.

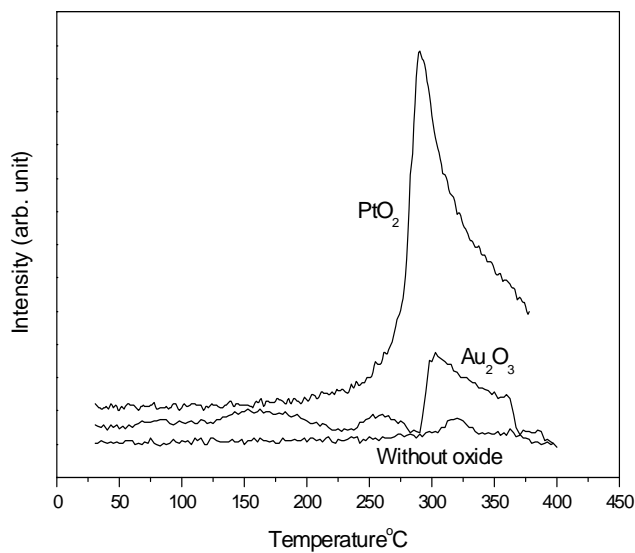


**Figure S12.** Comparing the MS ion current for the evolution of CO<sub>2</sub> due to the reaction of PTFE with PtO<sub>2</sub>, Au<sub>2</sub>O<sub>3</sub> and PTFE without oxide.

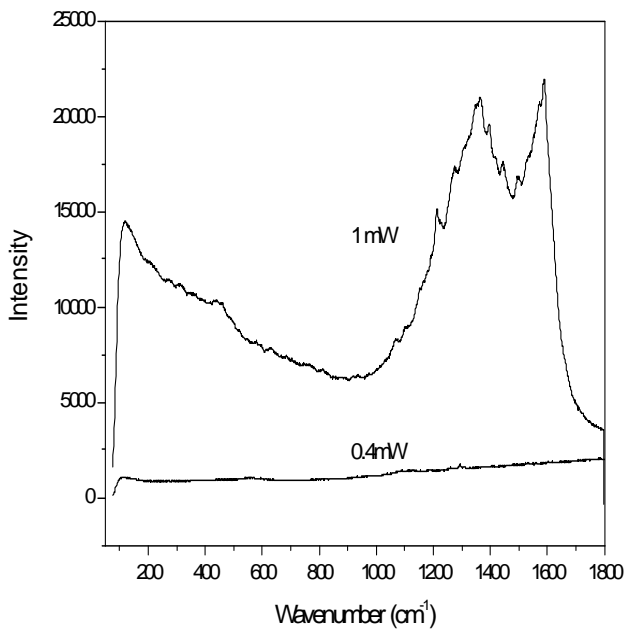


**Figure S13.** Raman Spectra of  $\text{Ag}_2\text{O}$ /polymer composites. The curves are due to the spectra of  $\text{Ag}_2\text{O}$ /(PE + Toluene) blend heated to  $80^\circ\text{C}$ . The laser intensities at the excitation wavelength of 632 nm were 0.13 and 0.32  $\text{kw}/\text{cm}^2$  respectively. At the laser power of 1mW, the black powder turned white.

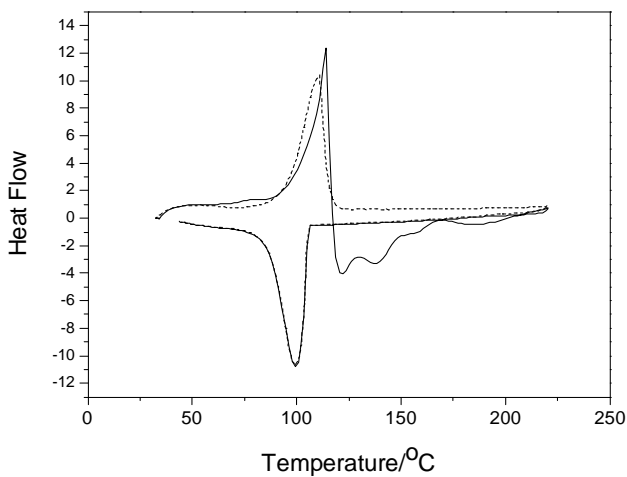


**Figure S14.** After the completion of the initial run ( $\text{Au}_2\text{O}_3/\text{PE}$ ): the exothermic reactions upon heating and re-solidification of the resulting melt, the second cycle shows melting of the remaining polymer, however no sign of further reaction was evident. Solid line – initial run, dotted line – second cycle.